Bull. Inst. Chem. Res., Kyoto Univ., Vol. 66, No. 2, 1988

Structure of PbSe-SnSe Artificial Superlattices

Zenji HIROI*, Noriaki NAKAYAMA* and Yoshichika BANDO*

Received April 25, 1988

Artificial superlattices (ASL) composed of PbSe and SnSe, $(PbSe)_m$ $(SnSe)_n$, have been characterized by X-ray diffraction. The two materials in their bulk forms possess different crystal structures and their lattice mismatch is fairly large. Structures of the ASL's are classified into four types depending on m and n; (I) Single crystalline ASL with orthorhombic SnS-type structure, (II) Single crystalline ASL with cubic NaCl-type structure, (III) ASL with transitional structures between I and IV, and (IV) ASL with the stacking of NaCl-type PbSe and SnS-type SnSe layers. Single crystalline ASL's (I and II) are stabilized when one constituent has its layer thickness less than a critical thickness which is independent of the counter layer thicknesses. The critical thicknesses are 1.8 nm (m=6) for I and 1.2 nm (n=4) for II. Pseudomorphic PbSe and SnSe layers are retained in the ASL's of I and II, respectively.

KEY WORDS: Superlattice/ PbSe-SnSe/ X-ray diffraction/ Pseudomorphic structure/

INTRODUCTION

Modern developments of the vapor phase deposition methods have made it possible to synthesize compositionally modulated films callde Artificial Superlattice (ASL). Various types of ASL's have been obtained by controlling the thicknesses of a couple of materials in an atomic scale. In paticular, there are a lot of work on ASL's composed of lattice-matched materials like GaAs-AlAs, which have shown that single-crystalline ASL's can be synthesized for such combinations.[1-3] From the viewpoint of creating new materials and new properties by constructing ASL structures, it is more interesting to choose lattice-mismatched materials. It may open a new field of matreial science to combine in an atomic scale two materials with different crystal structures and properties. There have been few reports, however, on the synthesis of such ASL's. We have tried to synthesize a coherent ASL composed of PbSe and SnSe.[4] PbSe has the cubic NaCl-type structure (O_h^5; $a \simeq a_c$), whereas SnSe has the orthorhombic SnS-type structure (D_{2h}^{16}; $a \simeq a_c/\sqrt{2}$, $b \simeq a_c/\sqrt{2}$, $c \simeq 2a_c$). Thick SnSe layers are known to grow on PbSe in the monolayer overgrowth mode with the orientation of

SnSe(001)//PbSe{100} and SnSe[100]//PbSe〈110〉.[5]

The lattice mismatch is fairly large: the misfit along $[100]_{SnSe}$ is 3.2%. The samples were designated as $(PbSe)_m(SnSe)_n$, implying m (001) atomic planes of PbSe and n (001) atomic planes of SnSe being stacked per modulation wavelength. As a result

* 広井善二, 中山則昭, 坂東尚周 : Laboratory of Solid State Chemistry, Institute for Chemical Research, Kyoto University, Uji, Kyoto 611.

of structural analysis by the x-ray diffraction (XRD) method and transmission electron microscopy (TEM) observations of the film cross-sections, it has been found that the desired structure whose compositional modulation is described by the step model can be obtained for a wide range of m and n. In this work, we report that four types of ASL's with different structures are formed depending on m and n, and discuss on their origins.

EXPERIMENTAL AND RESULTS

Samples were grown by evaporating PbSe and SnSe in a high vacuum (2×10^{-6} torr) onto hot (150°C) NaCl (001) substrates which were cleaved in the air and subsequently set in the vacuum chamber.[4] The growth rate was less than 0.1 nm/s. The structure of the obtained films was examined by XRD measurements. A conventional 2-axis and a 4-axis diffractometers were used with Cu-Kα radiation monochromatized by a pyrolytic graphite crystal. Diffraction patterns with the scattering vector normal to the film plane was measured by the former in the $\theta-2\theta$ scan mode to determine the crystal structure of the film. The latter was used to characterize the crystallinity of the films. X-ray intensity distributions around the (004) fundamental reflection of the NaCl-type structure in the (010)* reciprocal lattice plane was measured by the mesh scan method.

The XRD patterns in the $\theta-2\theta$ scan mode were generally composed of strong and sharp fundamental reflections, indexed as the (00L) reflections of the NaCl-type structure, and superlattice reflections originated from the artificial periodicities. Concerning the intensities and the peak widths of the (001) fundamental reflection, the XRD patterns were classified into three types. Figure 1 displays typical XRD patterns obtained from samples with (m, n)=(3, 3), (8, 4), and (13, 14). The peaks at L=1 and 2 are the fundamental (001) and (002) reflections of the NaCl-type structure, respectively. Superlattice reflections are clearly detected between them. The artificial superlattice periods corresponding to the sum of the individual PbSe and SnSe layer thicknesses are calculated to be 1.82 nm, 3.46 nm, and 8.00 nm for (m,n)=(3,3), (8,4), and (13,14), respectively. An essential point discriminating the three XRD patterns is the appearance of the (001) reflection. That of $(PbSe)_3(SnSe)_3$ is very strong and sharp, but it broadens for $(PbSe)_{13}(SnSe)_{14}$. Moreover, it can never be found in $(PbSe)_8(SnSe)_4$. Since the (001) reflection is forbidden for the NaCl-type structure, $(PbSe)_8(SnSe)_4$ is considered to have a NaCl-type ASL structure. On the other hand, the sharp (001) reflection of $(PbSe)_3(SnSe)_3$ indicates that this sample has a SnS-type ASL structure. The broadening of the (001) reflection implies an incoherent ASL structure including some structural imperfections around the interfaces as will be discussed later. These results imply that both the PbSe and SnSe layers can change their structures between the NaCl-type and the SnS-type depending on m and n.

The average interplanar spacing was calculated from the position of the (002) fundamental reflection for various combinations of m and n, and is plotted against PbSe content in Fig. 2. The data points fall on three straight lines, each following

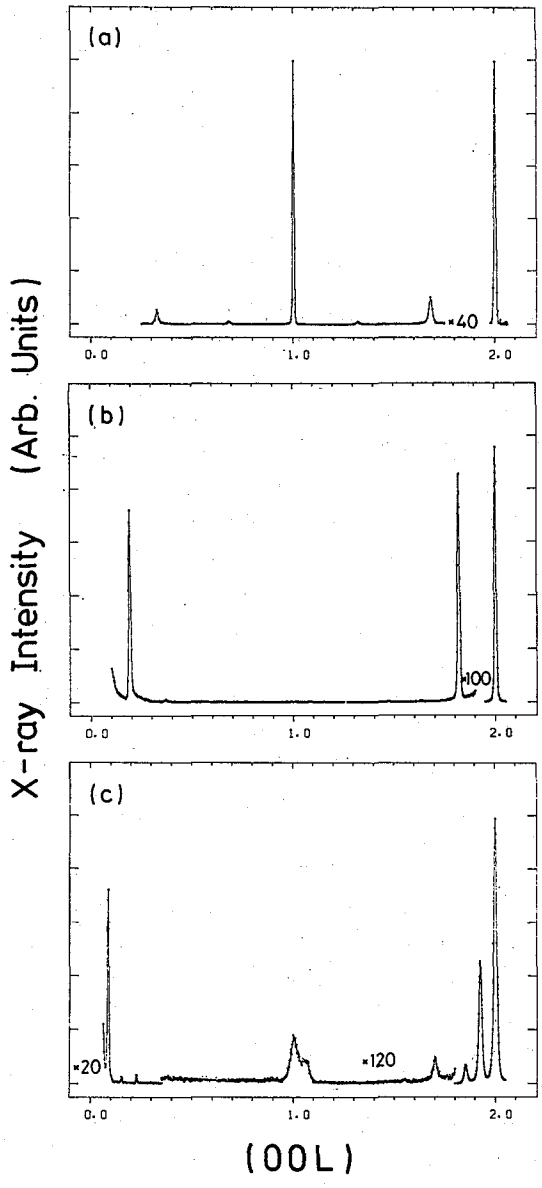

Fig. 1. X-ray diffraction patterns with the scattering vector normal to the film plane of (a) $(PbSe)_3$ $(SnSe)_3$, (b) $(PbSe)_8$ $(SnSe)_4$ and (c) $(PbSe)_{13}$ $(SnSe)_{14}$. These samples are typical ones for regions I, II and IV in the sample map shown in Fig. 3.

the Vegard's law. The values of d(002) extrapolated to PbSe contents of 0 and 100% are given in Table I, which correspond to the interplanar spacings in the SnSe and PbSe layers, respectively. Marks I-IV given in Fig. 2 and Table I refer to the four regions in a sample map to be shown in Fig. 3. As for the composition dependence of d(002), samples in regions III and IV show the same behavior. In comparison with the bulk values of 0.306 nm for PbSe and 0.289 nm for SnSe, serious deviations

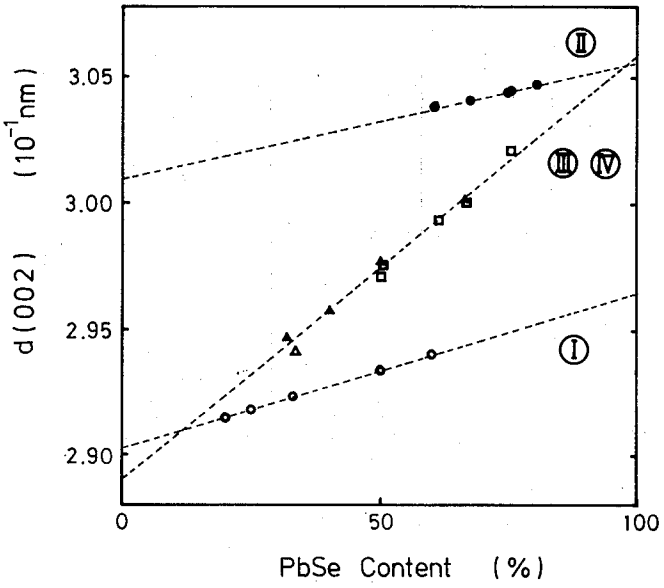

Fig. 2. Average interplanar spacing, d(002) vs. PbSe content for samples with various m and n. The data points fall on three straight lines. The values of d(002) extrapolated to PbSe contents of 0 and 100% are given in Table I, which correspond to the interplanar spacings in the SnSe and PbSe layers, respectively.

Table 1 Characteristics of samples in the four regions of the sample map.

Type	Fundamental reflection		Rocking curve of $(002)_c$	Interplanar spacing (nm)		Crystal structure	
	$(001)_c$	$(002)_c$		PbSe	SnSe	PbSe	SnSe
I	Sharp	Sharp	Sharp	0.2964	0.2902	SnS-type	SnS-type
II	—	Sharp	Sharp	0.3056	0.3010	NaCl	NaCl
III	Sharp	Sharp	Broad	0.3060	0.2893	SnS	SnS
IV	Broad	Sharp	Broad	0.3060	0.2893	NaCl	SnS

in regions I and II, namely, a 3% compression of PbSe in region I and a 4% elongation of SnSe in region II, are to be noted, while both the constituents keep their bulk values in regions III and IV.

The four sample regions are shown in Fig. 3 as a sample map in the m-n space. Crystallographic features are listed in Table I. The XRD patterns of (m, n)=(3, 3), (8, 4) and, (13, 14) shown in Fig. 1 are typical ones for regions I, II, and IV, respectively. That of region III is similar to that of region I, but the composition dependence of the average lattice spacing of region III differs from that of region I. It is worthy to point out that the boundaries determined by the appearance of the (001) peak and those determined by the interplanar spacing coincide exactly. Regions I and II are separated by a border line of n=(2/3)m, and a sample with (m, n)=(3, 2) just on the line shows an overlap of the two kinds of XRD patterns. It is surprising that the structure changes drastically by changing m and n by the minimum

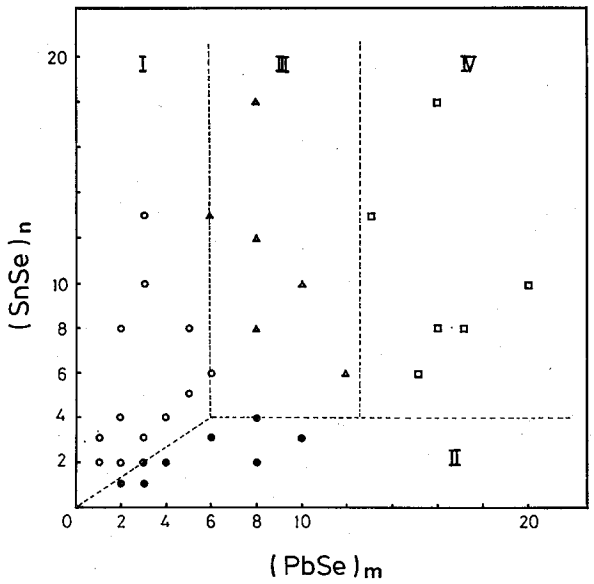

Fig. 3. Sample map in the m-n space. There are four regions divided by the broken lines which are determined by the appearance of the (001) fundamental reflection and the interplanar spacing of each layer. Typical structural features of each region are given in Table I.

unit. This is a strong suggestion of the accurately controlled monolayer deposition on sample preparation.

In order to examine the crystallinity of the films, the two-dimensional distribution of the X-ray diffracted beam intensity around the (004) fundamental reflection in the (010)* reciprocal lattice plane was measured. The results are shown in Fig. 4 as contour maps of the X-ray intensity. The samples of (m, n)=(8, 4), (3, 3), (7, 7) and (16, 18) represent those in regions II, I, III and IV in the sample map, respectively. The satellite reflections are also found in Fig. 4(d). It is obviously recognized that the intensity distribution is elongated along the [100]* direction for the samples in regions III and IV, which implies a short coherent length in the film plane of about 3 nm. Those peaks show no tendencies to spread into an arc shape. Therefore, the origin of the observed elongation may not be the crystal mosaicity which usually occurs as a result of the nucleation growth, but the loss of in-plane coherency due to the lattice imperfections introduced at the interfaces like misfit dislocations. On the other hand, the samples in regions I and II show a narrow intensity distribution both along the [100]* and [001]* directions, which confirms that the films in regions I and II are single-crystalline ASL's without any structural imperfections at the interfaces. Such a difference of the crystallinity highly correlates with the structural change depending on m and n, as discussed below.

DISCUSSION

It has generally been thought that, in the monolayer overgrowth mode, an

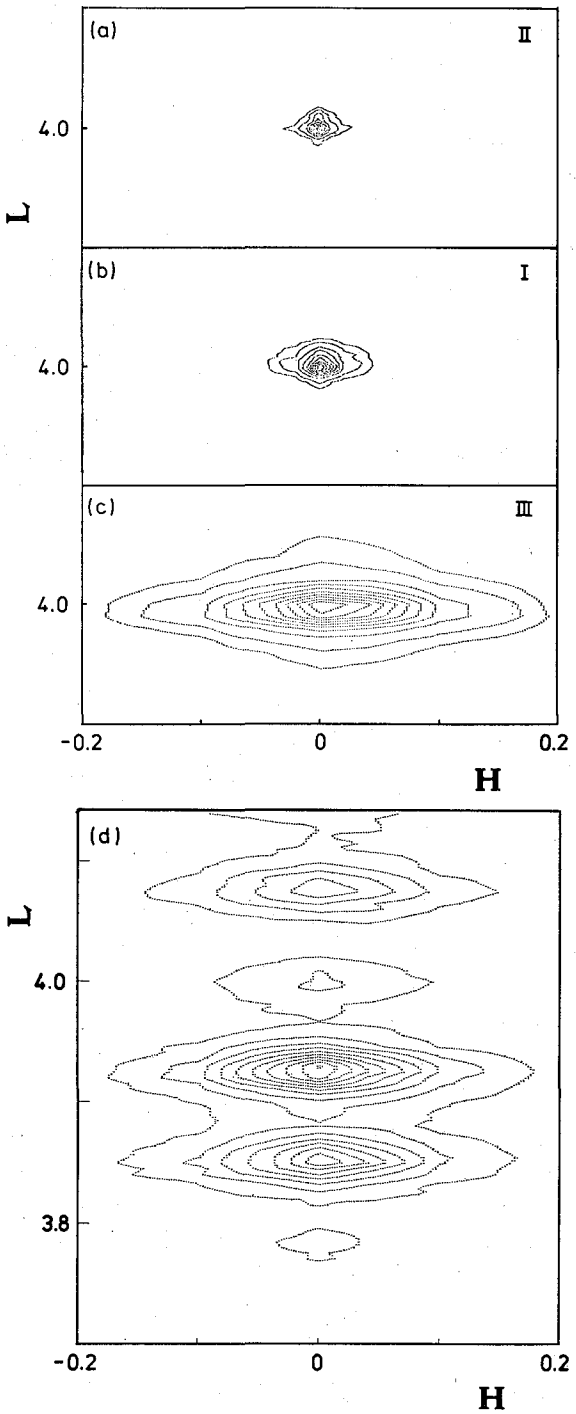

Fig. 4. Contour maps showing the intensity distributions of the (004) fundamental reflection in the (010)* reciprocal lattice plane for (a) $(PbSe)_8(SnSe)_4$, (b) $(PbSe)_3(SnSe)_3$, (c) $(PbSe)_7(SnSe)_7$ and (d) $(PbSe)_{16}(SnSe)_{18}$. These samples are representative ones in regions II, I, III and IV of the sample map, respectively.

epitaxial thin film can stabilize itself by accomodating the mismatch with the substrate by an elastic distortion while it is thin, but by formation of misfit dislocations when it exceeds a certain critical thickness (h_c). In some cases, it has been reported that such an elastic distortion leads to a pseudomorphic structure in the overgrowth layer. Yagi et al.[5] suggested from observations of misfit dislocations by TEM that SnSe grows on PbSe in this pseudomorphic growth mode, but the formation of the pseudomorphic layer has not been confirmed yet directly. Though the growth process of the PbSe-SnSe ASL is much more complicated because of the successive growth of two materials, it is reasonable to assume that, in region IV, the pseudomorphic structures of the overgrowth layers are unstable and they relax back to their natural structures by introducing misfit dislocations in the growth process. In addition, the broad (001) peak has been considered to suggest the formation of thin strained layers around the interfaces as discussed in ref. 4. Therefore, the coherency strain between the two layers seems to be released by the formations of both misfit dislocations and thin strained layers around the interfaces. That is, thick constituent layers have their natural structures and natural interplanar spacings except in the vicinity of the interfaces. The elongated (004) reflection shape observed for the sample in region IV implies an incoherent ASL structure as mentioned above. In order to get microscopic information on the interface structure, direct observations of the film cross-section by high-resolution TEM are in progress. On the other hand, when PbSe layers get thinner than 6 atomic layers ($m \leqq 6$) or SnSe layers become less than 4 atomic layers ($n \leqq 4$), they can keep the pseudomorphic structures. Thus, the lattice is constructed coherently through the interface. As a result, single-crystalline ASL's with the SnS-type structure can be formed in region I and those with the NaCl-type structure in region II. In other words, the structural phase transition of PbSe happens in region I and that of SnSe in region II, keeping the crystal structure of the other constituent unchanged. This is the reason why the (001) peak was observed in region I, while not in region II. The h_c's in the ASL structure for PbSe and SnSe may thus be determined as 1.8 nm and 1.2 nm, respectively. It is noted that those values are independent of the counter layer thicknesses. As a result of the structural phase transition, PbSe was contracted by 3% in region I, while SnSe was elongated by 4% in region II. Region III may have an intermediate structure between I and IV, because it showed a sharp (001) peak like that of region I but no changes in the interplanar spacings as observed in region IV. The difference of the crystallinity deduced from the (004) reflection shape is consistent with above discussions. The narrow spot-like shape observed for the samples in regions I and II strongly indicates that a perfectly coherent structure can be formed.

The values of h_c of 1.8 nm for PbSe and 1.2 nm for SnSe are much smaller than those found in other semiconductor systems. For example, Matthews et al.[6] determined it to be 35 nm experimentally for the GaAs-Ga ($As_{0.5}P_{0.5}$) system with a lattice mismatch of 1.8%. Reasons for the small h_c's in the present system may be the larger lattice mismatch and the different crystal symmetries of the constituents.

In comparison with the cases of GaAs-AlAs and others, in which both the constituents are distorted from cubic to tetragonal,[7] the thickness dependent structural changes of the constituent layers of the present system are of quite a different nature in the sense that these are far from a simple elastic distortion. The structural transitions of the constituent layers should induce a much more important change in the electronic band structure in the present system. The observed structural phase transitions can be interpreted as a positive proof of the pseudomorphic growth both in the PbSe/SnSe and SnSe/PbSe systems.

It is interesting to compare the sample map with an equilibrium pseudobinary PbSe-SnSe phase diagram.[8] There is a gap of miscibility for about $0.2<x<0.6$, where x is the mole fraction of PbSe. In the miscibility gap, the (Pb, Sn)Se alloys crystallizing in the NaCl and SnS-type structures coexist. The line of $n=(2/3)m$ which separates regions I and II in Fig. 3 coincides with that of $x=0.6$ which divides the cubic phase and the two-phase region in the equilibrium phase diagram. Nevertheless, instead of the two-phase region, one-phase with the orthrohombic symmetry was obtained in region I. This must be because the ASL was synthesized under a non-equilibrium condition. In contrast to those in regions III and IV, ASL's in regions I and II are, in a strict sense, superlattices with definite crystal symmetries and one-dimensional cation orderings. The slopes of d(002) for regions I and II in Fig. 2 are similar to those observed for the solid solutions. Therefore, local atomic structures arround Pb and Sn atoms seem to be similar to those in the bulk alloys.

In conclusion, structural properties of artificial superlattices composed of PbSe and SnSe have been investigated by the XRD method. It was found that four types of ASL's with different crystal structures are formed depending on m and n. As a result of the structural phase transition of one constituent, the single-crystalline and coherent ASL's are stabilized when PbSe or SnSe layers are thinner than a critical thickness. The critical thicknesses, at which the pseudomorphic structure relaxes back to its natural structure in the ASL, were found to be 1.8 nm for PbSe and 1.2 nm for SnSe.

This work was partially supported by a grant-in-aid for scientific research from the Ministry of Education, Japan. Useful discussions with M. Takano are acknowledged.

REFERENCES

(1) A. C. Gossard, P. M. Petroff, W. Wiegmann, R. Dingle, and A. Savage, *Appl. Phys. Lett.*, **29**, 323 (1976).
(2) P. M. Petroff, A. C. Gossard, W. Wiegmann, and A. Savage, *J. Cryst. Growth*, **44**, 5 (1978).
(3) L. L. Chang, A. Segmuller, and L. Esaki, *Appl. Phys. Lett.*, **28**, 39 (1976).
(4) Z. Hiroi, N. Nakayama, and Y. Bando, *J. Appl. Phys.*, **61**, 206 (1987); *Bull. Inst. Chem. Res., Kyoto Univ.*, **64**, 259 (1986).
(5) K. Yagi, K. Takayanagi, Y. Matsushita, and G. Honjo, *J. Cryst. Growth*, **24/25**, 307 (1974).
(6) J. W. Matthews and A. E. Blakeslee, *J. Cryst. Growth*, **32**, 265 (1976).
(7) J. M. Brown, N. Holonyak, Jr., M. J. Ludowise, W. T. Dietze, and C. R. Lewis, *Appl. Phys. Lett.*, **43**, 863 (1983).
(8) T. C. Harman, I. Melngailis, *Appl. Solid State Science*, **4**, 1 (1974).